tvst

https://doi.org/10.1167/tvst.8.6.19

Article

Objective Measurement of Local Rod and Cone Function Using Gaze-Controlled Chromatic Pupil Campimetry in Healthy Subjects

Carina Kelbsch[1,2], Katarina Stingl[2], Melanie Kempf[2], Torsten Strasser[1,3], Ronja Jung[1], Laura Kuehlewein[2,3], Helmut Wilhelm[1,2], Tobias Peters[1], Barbara Wilhelm[1], and Krunoslav Stingl[1,2]

[1] Pupil Research Group, Center for Ophthalmology, University of Tuebingen, Tuebingen, Germany
[2] University Eye Hospital, Center for Ophthalmology, University of Tuebingen, Tuebingen, Germany
[3] Institute for Ophthalmic Research, Center for Ophthalmology, University of Tuebingen, Tuebingen, Germany

Correspondence: Katarina Stingl, Center for Ophthalmology, University of Tuebingen, University Eye Hospital, Elfriede-Aulhorn-Str. 7, Tuebingen, 72076, Germany. e-mail: katarina.stingl@med.uni-tuebingen.de

Received: 15 May 2019
Accepted: 2 September 2019
Published: 20 November 2019

Keywords: rod function; cone function; pupillary responses; pupil campimetry; objective evaluation of local retinal function; eccentricity effect

Citation: Kelbsch C, Stingl Ka, Kempf M, Strasser T, Jung R, Kuehlewein L, Wilhelm H, Peters T, Wilhelm B, Stingl Kr. Objective measurement of local rod and cone function using gaze-controlled chromatic pupil campimetry in healthy subjects. Trans Vis Sci Tech. 2019;8(6):19, https://doi.org/10.1167/tvst.8.6.19

Purpose: We introduce a new approach for functional mapping of rod and cone activity by measuring pupillary responses to local stimulation via gaze-controlled chromatic pupil campimetry (CPC).

Methods: Pupillary constriction amplitude and latency to constriction onset to local photopic and scotopic light stimuli at different locations within the 30° central visual field were analyzed in 14 healthy subjects (4 males, 34 ± 11 years, mean ± standard deviation [SD]). All subjects were measured twice for evaluating the test–retest variability and reproducibility of the method.

Results: For the cone-favoring protocol (ConeProt), the relative maximal constriction amplitude was most pronounced in the center (26.8% ± 6.3%) with a hill-shaped decrease from the fovea to the periphery. For the rod-favoring protocol (RodProt), it was smaller (center, 13.5% ± 4.5%) with a profile lacking the central peak. Mean latency to constriction onset was faster for cones (277 ± 25 ms) than for rods (372 ± 13 ms). Mean intraclass correlation at the different stimulus locations was 0.84 ± 0.08 for RodProt and 0.75 ± 0.11 for ConeProt; mean coefficients of repeatability value of all stimulus locations was 5.9% ± 1.2% and 8.6% ± 1.7%, respectively.

Conclusions: CPC provides an objective evaluation of local rod and cone function within the central 30° visual field. It shows a photoreceptor-specific profile in healthy subjects. Due to its easy, noncontact, gaze-controlled character, it is a clinically applicable method and may fill the gap of functional diagnostics of rods and cones of the human retina.

Translational Relevance: Chromatic pupil campimetry provides information about the local rod and cone function of the human retina with distinct pattern of distributions in an objective manner.

Introduction

Measuring local cone and rod function of the human retina still remains a methodologic challenge. Regarding cone function, classical visual field performance is the gold standard in clinical daily routine, but is vulnerable to the subjects' compliance due to its subjective character and losses in validity with increasing visual impairment. Multifocal electroretinography is another method currently applied for testing central local cone function, but requires accurate fixation, which is challenging with increasing visual impairment[1] and/or low compliance. Another attempt to measure the integrity of foveal cones is to use the optical Stiles-Crawford effect.[2] Estimating local rod function is even more difficult; to our knowledge no objective test is available currently for that purpose. Dark-adapted chromatic perimetry has

potential, but also shortcomings due to its subjective and extremely time-consuming character and its dependency on an accurate fixation.[3]

Using pupillary responses to light stimulation provides an easy, rapid, noncontact, and most importantly, an objective method to estimate retinal function. In healthy human subjects, pupillary light responses are composed of responses from rods (rhodopsin-driven), S-/M-/L-cones (opsin-driven), and intrinsically photosensitive retinal ganglion cells (ipRGCs; melanopsin-driven). By presenting light stimuli of varying intensity, duration, and wavelength, combined with specific backgrounds (e.g., rod-suppressing background) and adaptation conditions, it is possible to stimulate rods, cones, or ipRGCs, even if a strict separation currently is not yet feasible (see prior review[4]). Several clinical studies have proven the suitability of chromatic pupillography to detect changes in specific ophthalmologic disorders, ranging from impaired ipRGC function in glaucoma,[5–9] age-related macular degeneration,[10–12] diabetes,[13,14] and seasonal affective disorders[15] to reduced rod/cone function with enhanced ipRGC function in hereditary rod-cone dystrophies. In retinitis pigmentosa, pupillary responses still are recordable, even in patients with extinguished electroretinography recordings.[16,17] Furthermore, protocols for chromatic pupillography have been developed for the objective assessment of efficacy in gene therapy in patients with *CNGA3*-linked achromatopsia.[18]

In contrast to a full-field stimulation, which was applied in all the aforementioned studies, pupil campimetry enables the examination of local function of the retina by specifically designed stimulation paradigms at different locations of the visual field.[19–24] We recently presented a new device for chromatic pupil campimetry (CPC) with implemented gaze tracking, which allows for precise retinotopic stimulation regardless of fixation problems, thereby overcoming one of the most relevant drawbacks of pupil campimetry.[25]

In the present study of healthy subjects, we introduced two pupillary stimulus protocols, suitable for clinical application, that assess the local functionality of either rods or cones. Additionally, we investigated the intraindividual test–retest variability, and the effect of stimulus eccentricity from the fovea on the pupillary responses, which is not yet sufficiently understood. Skorkovská et al.[26] demonstrated a clear reduction of the pupillary constriction amplitude in the peripheral compared to the central retina to white stimulation; however, such an "eccentricity effect" could not be observed by Joyce et al.[27] under dark-adapted conditions comparing pupillary responses at 0° and 20° of retinal eccentricity.

To date, to our knowledge no systematic investigation of the distribution pattern of pupillary responses to local retinal stimulation, favoring either rods or cones, has been presented; thus, this study is the first to address this fundamental question.

Methods

Participants and Ethics

A total of 14 adult healthy subjects (4 males, 10 females; mean age, 34 ± 11 standard deviation [SD] years) volunteered to participate in the study after detailed information was provided and written informed consent had been given. The study was approved by the local institutional ethics committee and followed the tenets of the Declaration of Helsinki. All participants underwent an ophthalmologic examination to exclude any possible interfering pathology. The ophthalmologic examination included visual acuity, swinging-flashlight test, slit-lamp examination, fundus ophthalmoscopy, 30° visual field examination (static automatic strategy, Octopus 101 or 900; Haag-Streit International, Wedel, Germany) and optical coherence tomography (Spectralis-OCT; Heidelberg Engineering GmbH, Germany) of the macular region.

Chromatic Pupil Campimetry (CPC)

The basic setup and software of our pupil campimeter have been described in detail previously.[25] The CPC setup used an OLED-monitor (Samsung/LG OLED 55C7V) for stimulus presentation, at a fixation distance of 40 cm from the subject's eye (campimetry = stimulus presentation on a flat monitor with stimulus size correction for distance; perimetry = stimulus presentation on a hemisphere bowl). An infrared camera recorded the pupil diameter continuously with a temporal resolution of 10 ms. The examination was performed in a completely dark and quiet room. The subject was seated comfortably in front of the monitor using a combined chin- and headrest for stabilization. A central dim fixation mark at the monitor supported a steady fixation. Furthermore, using gaze-tracking, the software automatically corrected subtle eye movements, ensuring a retinotopic stimulus presentation, which is particularly important in subjects with

Figure 1. Pupil campimetry setup. Stimulus presentation on an OLED monitor (A). Examiner's monitor with stimulation details and pupil tracking (B). Result from a normal subject; cone protocol (C). The size of the squares represents the amplitude of pupil constriction after the respective local light stimulation. *Color scale* indicates deviation from mean of the group from *green* to *red*.

central impaired vision or mild-to-moderate nystagmus. Before the actual experiment, a short calibration using a fixation mark in each quadrant was performed to ensure a reliable individual gaze-tracking.

In this study, we randomly selected and measured one eye per participant. For the test, one eye was patched, while the other eye was stimulated and the respective direct pupillary response was measured. Figure 1 shows a sketch of the CPC setup with exemplary results from a healthy subject.

Stimuli were presented at different locations within the 30° central visual field and were adjusted in size, intensity, color and duration. Background illumination and adaptation status of the retina were likewise selected according to the specific protocols. Each location was tested two (ConeProt) or four (RodProt) times and the mean value of the pupillary responses was calculated. In case of strong artefacts (e.g., severe blinking during stimulus presentation), the stimulus was repeated automatically. To ensure a stable baseline for each stimulus, stimuli were repeated if at least 90% of the initial pupil diameter was not reached. The examination per protocol lasted approximately 6 to 8 minutes, depending on the used protocol and the subjects' compliance (e.g., blinking).

Pupillographic Protocols

Cone-Favoring Protocol (ConeProt)

After 5 minutes of adaptation time to a dim blue background (0.01 cd/m^2; wavelength 460 nm ± 30 nm full width at half maximum [FWHM]; ≙ 2.1×10^{-8} Watt) for the partial saturation of rods without reducing the baseline diameter too much, red stimuli were presented on the same dim blue background on a total of 41 locations from central (0°) to 30° eccentricity in a randomized order (baseline period, 500 ms; stimulus radius, 3°; stimulus duration, 1 second; stimulus intensity, 60 cd/m^2; stimulus wavelength, 620 ± 30 nm FWHM; ≙ 1.7×10^{-5} Watt; interstimulus interval, 4 seconds; two repetitions per location).

Rod-Favoring Protocol (RodProt)

The ConeProt subsequently was followed by a dark-adaptation time of 20 minutes. Then, dim blue stimuli were presented at 33 locations within the central 30° of the visual field in a randomized order (baseline period, 500 ms; stimulus radius, 5°; stimulus duration, 100 ms; stimulus intensity, 0.01 cd/m^2; stimulus wavelength, 460 ± 30 nm FWHM; ≙ 2.1×10^{-8} Watt; interstimulus time, 2 seconds; four repetitions per location).

Adaptation and stimulus conditions of the different protocols can be seen in chronological order in Figure 2. The whole experiment lasted approximately 45 minutes.

Statistics

Measurements and evaluations were performed in left eyes of 10 subjects and in right eyes of four subjects. The pupillary responses of all measured right eyes were mirror-converted to left eyes to control for temporal-nasal consistency. Artefact elimination was done by detecting eye blinks based on the change in standard deviation and removed by a linear interpolation (for more details see the study of Stingl et al.[25]).

Data are presented in absolute values (absolute pupil diameter in millimeters) and normalized to the baseline pupil diameter (relative pupil constriction amplitude to baseline in percent) using Equation 1:

$$amplitude_{rel}(t) = \frac{baseline - amplitude_{absolute}(t)}{baseline} * 100 \quad (1)$$

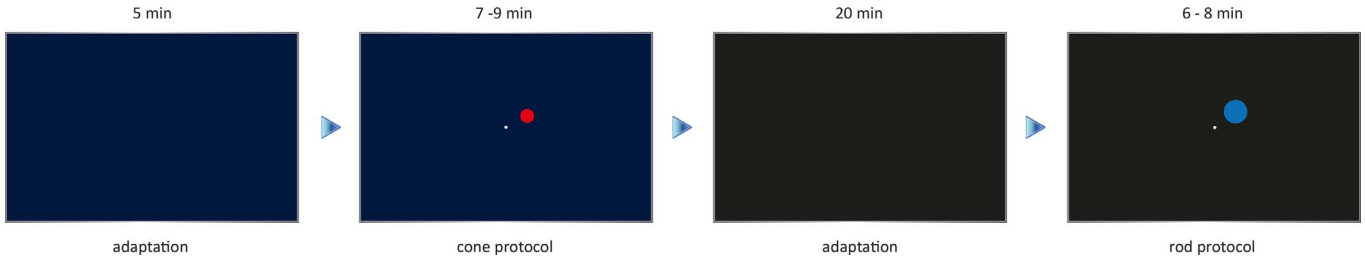

Figure 2. Chronological order of the experiment consisting of two pupillographic protocols with one stimulus location exemplified and background adaptation periods.

The baseline pupil diameter was calculated as the mean of the 500 ms prestimulus time.

Primary pupillary outcome parameters were the maximal constriction amplitudes for each stimulus location. Topologies of the relative pupil constriction amplitudes were created to visualize the pattern of distribution in relation to the eccentricity from the center.

Additionally, the latency to constriction onset was calculated by fitting a line to the linear part of the pupillographic curves between 400 and 600 ms after stimulus onset for each recording and intersecting it with the baseline.

Coefficient of Repeatability (CoR) values were calculated to determine the range of repeatability and reproducibility at all stimulation locations.[28]

To test the overall test–retest reliability of the method, we used intraclass correlation.[29,30] All analyses were performed in Matlab (MathWorks, Inc., Natick, MA).

Results

Baseline Pupil Diameter

During the cone condition, mean baseline pupil diameter was 6.1 ± 0.8 mm (mean ± SD). During the rod condition after dark-adaptation, mean baseline pupil diameter was 6.7 ± 0.7 mm.

Maximal Constriction Amplitude and Pattern of Distribution (Eccentricity Effect)

For the ConeProt, the maximal constriction amplitude was most pronounced in the center of the retina (1.65 ± 0.4 mm; 26.8% ± 6.3%) with a hill-shaped decrease with increasing eccentricity from the fovea (Figs. 3A, 4A).

For the RodProt, the maximal constriction amplitude was expectedly smaller (center, 0.89 ± 0.25 mm; 13.5% ± 4.5%) with a distinct pattern of distribution, lacking the central peak of the cone-favoring pupillary responses (Figs. 3B, 4B).

Latency to Constriction Onset

A comparison of the results of cone- versus rod-specific stimulation revealed a shorter latency to constriction onset for cones than for rods. For the ConeProt, mean latency to constriction onset was 277 ± 25 ms (range, 222–334 ms) with increasing latencies to more peripheral stimuli. For the RodProt, mean latency to constriction onset was 372 ± 13 ms (range, 340–390 ms) with similarly increasing latencies to more peripheral stimuli (Fig. 5).

Reliability and Repeatability of Cone and Rod Driven Pupil Responses

To test the overall test–retest reliability of the method, we used intraclass correlation (ICC). Mean value of ICC at the different stimulation locations was 0.75 ± 0.11 (range, 0.44–0.92) for ConeProt and 0.84 ± 0.08 (range, 0.62–0.96) for RodProt. The ICC did not indicate any specific differences of the reliability over the different test locations in both protocols.

The CoR were calculated according to the proposal from Bland and Altman[27] per stimulus location and separated for the cone and rod protocols. They served to estimate the range of repeatability and reproducibility at all stimulation locations. Mean CoR value of all stimulus locations was 8.6% ± 1.7% for ConeProt and 5.9% ± 1.2% for RodProt. This means that the observed change in the pupillary responses in the test–retest data was less than the reported CoR value for 95% of the subjects. Or conversely, for example during clinical application in the follow-up examination of a patient, a change in the pupillary retest responses that exceeds these CoR values has a probability of 95% to be a genuine change.

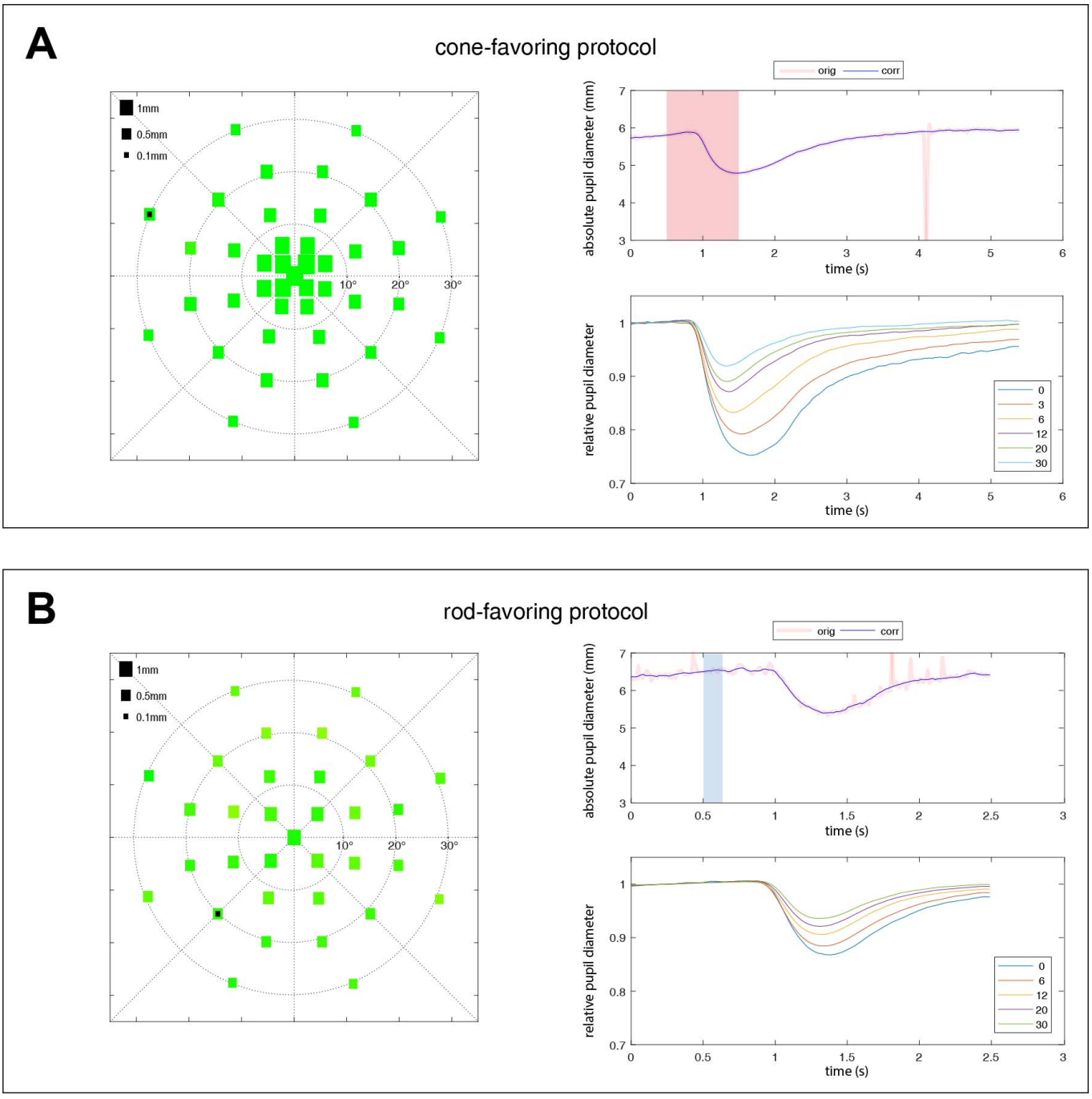

Figure 3. Averaged pupillary responses over all subjects ($n = 14$) for the cone (A) and rod (B) protocols. The *left column* shows the averaged absolute values of the maximal constriction amplitudes. The size of the squares represents the amount of pupil constriction (in mm) after the respective local light stimulation. The *right column* shows the raw data of one exemplary pupillographic trace (*upper right column*). Stimulus presence is indicated as shaded *red* (cone) or *blue* (rod) areas. The location of that exemplary trace is marked by a *black square* on the scatter plot on the *left side*. The averaged relative pupillary traces corrected for baselines and sorted by their eccentricity from the center with 0° to 30° are presented in the *lower right column*.

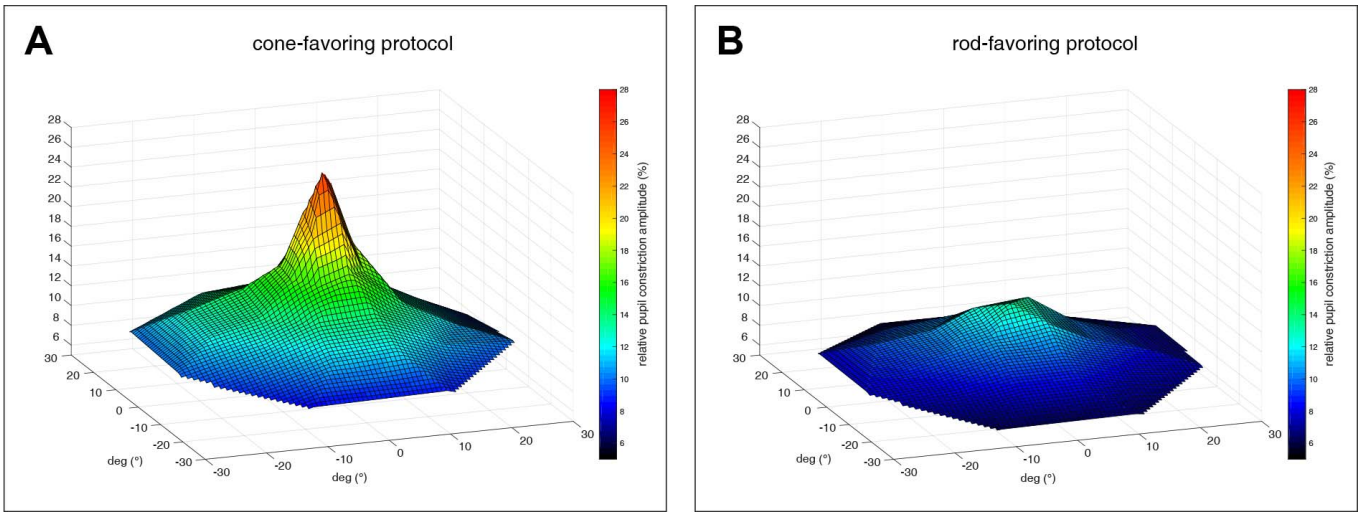

Figure 4. Topology of pupillary responses (relative pupil constriction amplitude in percent from baseline) for cone- (A) and rod- (B) favoring stimulations; average over all subjects ($n = 14$).

Proof of Concept of the Protocols in Hereditary Retinal Degenerations

As a proof of concept of the photoreceptor-specific stimulation of our protocols, we examined exemplarily two patients lacking cell-specific retinal neurons: one patient suffering from retinitis pigmentosa with confirmed *PDE6A*-mutations (Fig. 6) and one patient with achromatopsia with confirmed *CNGA3*-mutation (Fig. 7). The first patient with absent rod function and impaired cone function revealed impaired responses to the central 15° of the visual field to ConeProt and no pupillary responses to RodProt. The patient with achromatopsia with nonfunctioning cones showed preserved responses to RodProt, and severely impaired responses to ConeProt, while these responses showed "rod-typical" time dynamics with a latency to constriction onset of 355 ms (rod protocol, 341 ms); thus, probably reflecting rod responses.

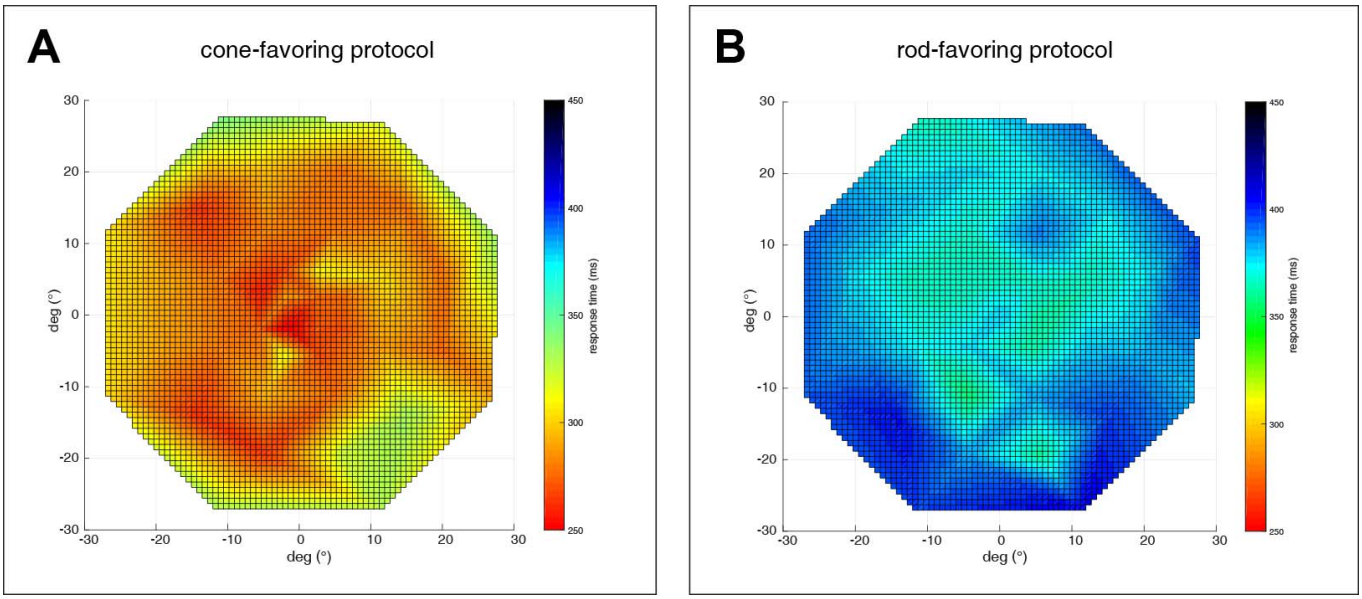

Figure 5. Latency to constriction onset. Maps of the stimulated 30° visual field. The color bar codes for the latency time (in ms) of pupillary responses to local stimulation favoring cones (A) or rods (B).

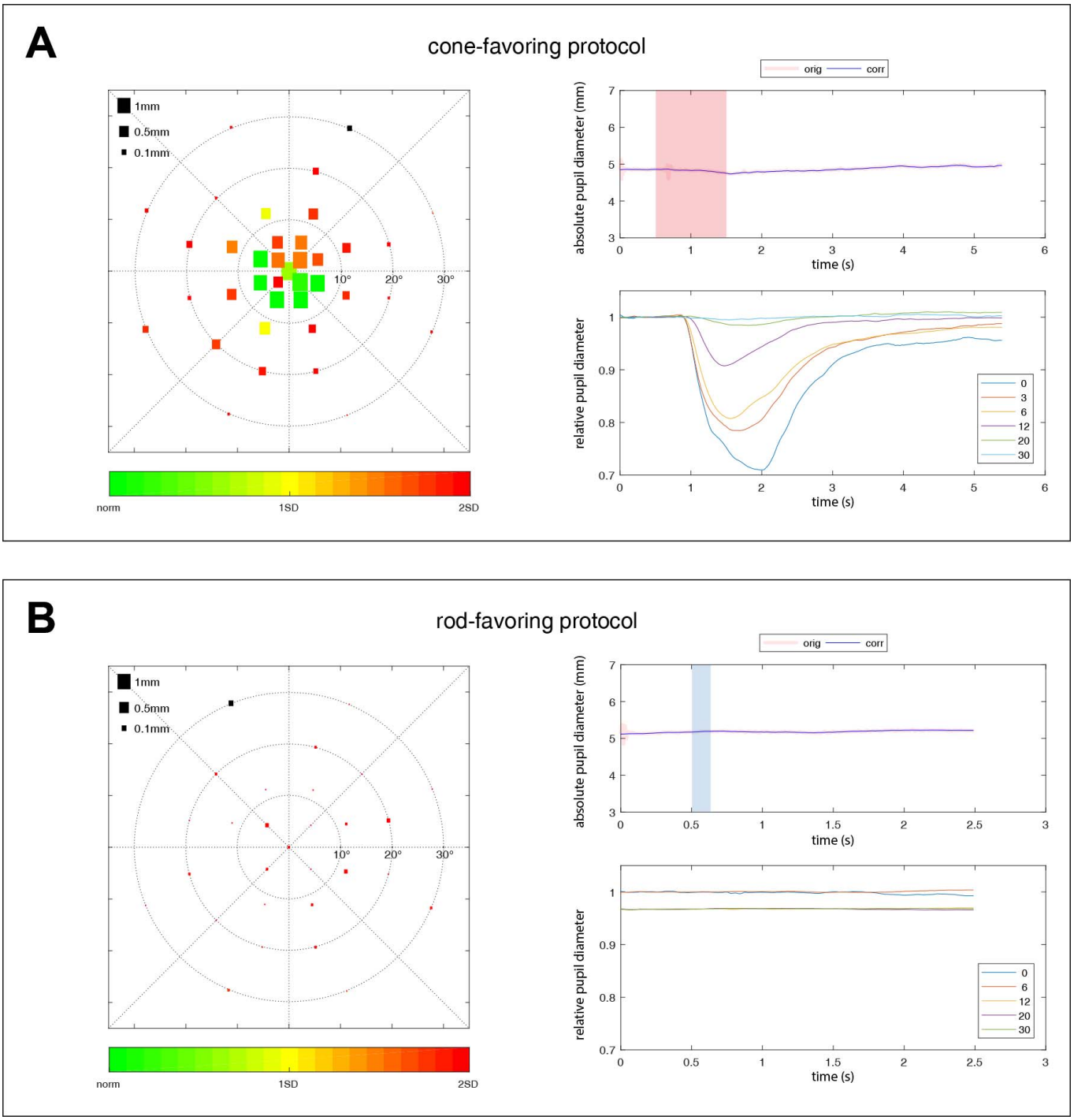

Figure 6. Exemplary pupillary responses for a patient suffering from retinitis pigmentosa with confirmed *PDE6A*-mutations with concentrically impaired cone responses to the central 15° of the visual field (A) and absent rod function (B). The size of the *squares* in the scatter plot on the *left* represents the amplitude of pupil constriction after the respective local light stimulation. Color scale indicates deviation from the mean of the healthy group from *green* to *red*. The *right column* shows the raw data of one exemplary pupillographic trace (*upper right column*). Stimulus presence is indicated as shaded *red* (cone) or *blue* (rod) areas. The location of that exemplary trace is marked by a *black square* on the scatter plot on the *left side*. The averaged relative pupillary traces corrected for baselines and sorted by their eccentricity from the center with 0° to 30° are presented in the *lower right column*.

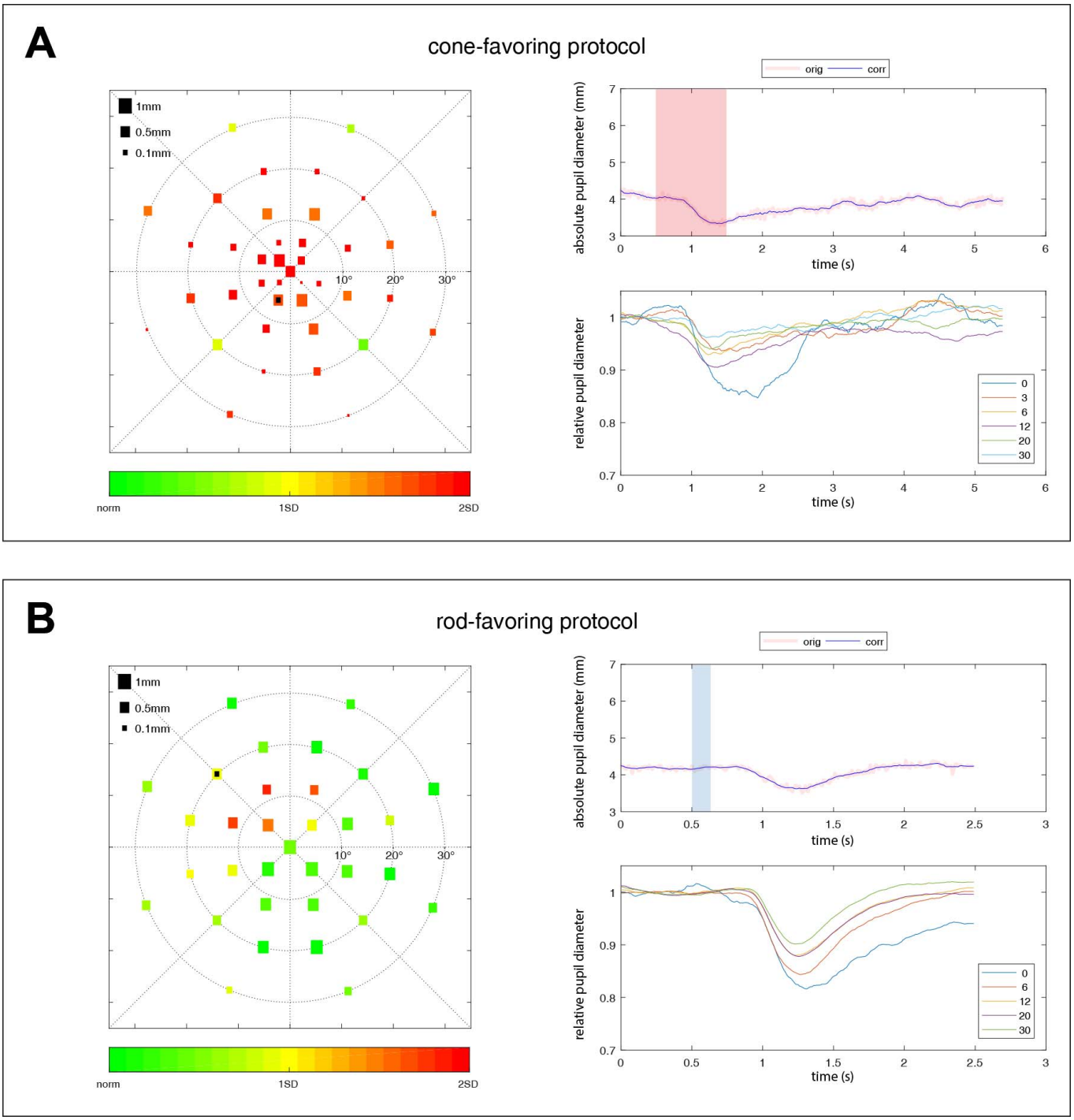

Figure 7. Exemplary pupillary responses for a patient suffering from achromatopsia with confirmed *CNGA3*-mutations showing severely impaired responses to the cone protocol following "rod-typical" time-dynamics (A) and preserved responses to the rod protocol (B). The size of the *squares* in the scatter plot on the *left* represents the amplitude of pupil constriction after the respective local light stimulation. Color scale indicates deviation from the mean of the healthy group from *green* to *red*. The *right column* shows the raw data of one exemplary pupillographic trace (*upper right column*). Stimulus presence is indicated as shaded *red* (cone) or *blue* (rod) areas. The location of that exemplary trace is marked by a *black square* on the scatter plot on the *left* side. The averaged relative pupillary traces corrected for baselines and sorted by their eccentricity from the center with 0° to 30° are presented in the *lower right column*.

Discussion

We addressed the clinically relevant methodologic lack of testing rod and cone function of the human retina topographically. Its clinical relevance is particularly evident, since the development of new techniques to restore some vision in severely visually-impaired patients. For example, in gene therapy trials, an unmet goal remains how to measure the remaining rod and cone morphology precisely and their function objectively in a severely degenerated retina before and after treatment.

We demonstrated that CPC as a diagnostic tool is able to provide information about local retinal function in an objective manner. The easy and noncontact characteristic of the method, together with the developed short-lasting protocols, either favoring the stimulation of rods or cones, renders CPC a clinically applicable method that can fill the gap of a missing objective evaluation of photopic and scotopic retinal function in humans. The implemented gaze-tracking ensures a retinotopic precise stimulation regardless of fixation difficulties.

Our results provided a systematic examination on the pattern of distribution and effect of eccentricity of pupillary responses to local retinal stimulation favoring either rods or cones and revealed a remarkably distinct topology of pupillary responses for the cone-specific and rod-specific stimulations (Fig. 4). For both stimulation paradigms, the maximal constriction amplitude was most pronounced in the center, but it was expectedly stronger for cones (ConeProt, 26.8% ± 6.3%; RodProt, 13.5% ± 4.5%; Fig. 3).[31] For cone-favoring stimulation, the constriction amplitudes, as a marker of sensitivity, showed a conspicuous hill-shaped topology with a symmetric decline with increasing eccentricity from the fovea. These results are in accordance with recent measurements of the distribution of cone density in adult healthy retinas using adaptive optics flood illumination.[32] Legras et al.[32] reported an approximately 50% reduction of cone density from 2° to 6° of eccentricity. Our data also matched with the term "hill of vision," which is used in standard visual perimetry to characterize the decreasing visual sensitivity under photopic conditions from the fovea to periphery.[33] However, in the RodProt, we observed a distinct pattern of a flatter, more homogeneous distribution, lacking the central peak of the ConeProt pupillary responses, and more specifically, only showing a minor peak within the central 10°. This profile is not representative of the rod cell distribution; however, we considered that the neuronal connectivity between rods and bipolar cells possibly contributed to the observed results. Our results provided an explanation for different findings regarding eccentricity effects under photopic and scotopic stimulation conditions due to different photoreceptor contributions, unifying results from previous studies.[26–27] These distinct photoreceptor-specific patterns could not be observed in a multifocal pupillographic approach. However, due to huge methodologic differences, it is hard to compare these two studies.[34]

The latency to constriction onset was faster for cones (277 ± 25 ms) than for rods (372 ± 13 ms), confirming complementary results for pupil campimetry with previous general statements.[35] The slower onset of the rod responses seems not to be related to the maximum size of pupillary constriction. For example, latency to constriction onset for central rods was much slower than for peripheral cones, although their amplitudes of constriction were similar in dimension.

It is well-known that pupillary responses underlie a certain intra- and interindividual variability. The intraclass correlation to test the overall test–retest reliability of the method, and the determination of the CoR confirmed a satisfactory reproducibility between two measurements of one subject, particularly for the RodProt where four repetitions per stimulus location were averaged (ConeProt two repetitions).

As a proof of concept of our developed protocols, we presented pupillary responses from two patients lacking opposite photoreceptor cell types. The first patient suffered from retinitis pigmentosa, a hereditary rod-cone dystrophy, due to *PDE6A*-mutations. The *PDE6A*-gene encodes the α-subunit of the rod photoreceptor cGMP-specific phosphodiesterase of the rod phototransduction cascade.[36] The absent rod function and impaired cone function with a concentrically affected decrease to the central 15° of the visual field could be depicted precisely by pupil campimetry (Fig. 6). As in the central visual field the pupillary response in ConeProt was preserved but, in the same position, the response in RodProt was totally absent, it demonstrated a strong photoreceptor-specific targeting achieved by our stimulus protocols. If this was not the case and, for instance, our rod-favoring stimuli led to substantial contribution from cones, then the pupillary responses to RodProt would not be negligible at the center.

This effective separation of rod function represents an important progress in comparison to stimulation

paradigms under mesopic conditions with an unavoidably mixed stimulation of rods and cones.[23,37]

By contrast, achromatopsia is characterized by nonfunctioning cones, in our patient induced by *CNGA3*-mutations encoding the α-subunit of the cyclic nucleotide-gated cation channel in cone photoreceptors leading to impairment in the cone phototransduction cascade, while rods are essentially preserved.[38] As expected our results showed preserved responses to RodProt (Fig. 7). Interestingly, pupillary responses to ConeProt were not absent, but showed severely impaired responses with "rod-typical" time dynamics with a latency to constriction onset of 355 ms (RodProt, 341 ms). We assumed that these pupillary responses reflect rod contributions based on hypersensitive rods lacking the physiologic inhibiting cone signals in achromatopsia. Similar findings could be observed for chromatic pupillography to full-field stimulation in a larger group of *CNGA3*-achromatopsia patients.[18]

There are limitations to our study. We are aware of the fact that the introduced protocols are a compromise between clinical applicability and currently known pure fundamental psychophysical features of human photoreceptors in complex laboratory conditions. With the used, relatively dim, background illumination, no full rod saturation can be expected, but a high-irradiance background would unavoidably lead to a strongly reduced baseline diameter without sufficient capability of a further constriction range to superimposed stimuli. Nevertheless, as the results of mean pupillary baseline diameter and maximal constriction amplitudes for ConeProt suggested enough range left before reaching the anatomical limits for constriction, we may slightly increase the background illumination in future applications. Likewise, as RodProt shows a higher precision compared to ConeProt, we plan to increase the number of repetitions per stimulus location for ConeProt in future applications. In this study, we did not examine the local function of ipRGCs as the OLED monitor could not provide optimal stimulation characteristics recommended for ipRGCs.[4] The focus of the study was on local photoreceptor function of the outer retina. Additional testing of local function of ipRGCs (inner retina) would definitely be worth addressing in future studies with methodologic improvement.

In conclusion, gaze-controlled CPC enables to test local rod and cone function in an objective manner and reveals pupillary responses as clinical read-outs for photoreceptor-specific patterns of distribution over the retina in healthy subjects.

Acknowledgments

The authors thank Irena Stingl for her graphical support with the figures and the RD-Cure Consortium for support in the organization of the patient with *PDE6A*-mutations. We acknowledge support by Open Access Publishing Fund of University of Tuebingen.

Supported by the Egon Schumacher-Stiftung, Barnstorf, Germany, a private foundation without commercial interest.

Previous oral presentation at the ARVO Annual Meeting, 2 May 2019, Vancouver, Canada.

Disclosure: **C. Kelbsch**, None; **Ka. Stingl**, None; **M. Kempf**, None; **T. Strasser**, None; **R. Jung**, None; **L. Kuehlewein**, None; **H. Wilhelm**, None; **T. Peters**, None; **B. Wilhelm**, None; **Kr. Stingl**, None

References

1. Hood DC, Odel JG, Chen CS, Winn BJ. The multifocal electroretinogram. *J Neuroophthalmol*. 2003;23:225–235.
2. Kanis MJ, Wisse RP, Berendschot TT, van de Kraats J, van Norren D. Foveal cone-photoreceptor integrity in aging macula disorder. *Invest Ophthalmol Vis Sci*. 2008;49:2077–2081.
3. Bennett LD, Klein M, Locke KG, Kiser K, Birch DG. Dark-adapted chromatic perimetry for measuring rod visual fields in patients with retinitis pigmentosa. *Transl Vis Sci Technol*. 2017;6:15.
4. Kelbsch C, Strasser T, Chen Y, et al. Standards in pupillography. *Front Neurol*. 2019;10:129.
5. Kelbsch C, Maeda F, Strasser T, et al. Pupillary responses driven by ipRGCs and classical photoreceptors are impaired in glaucoma. *Graefes Arch Clin Exp Ophthalmol*. 2016;254:1361–1370.
6. Feigl B, Mattes D, Thomas R, Zele AJ. Intrinsically photosensitive (melanopsin) retinal ganglion cell function in glaucoma. *Invest Ophthalmol Vis Sci*. 2011;52:4362–4367.
7. Najjar RP, Sharma S, Atalay E, et al. pupillary responses to full-field chromatic stimuli are reduced in patients with early-stage primary open-angle glaucoma. *Ophthalmology*. 2018;125:1362–1371.

8. Adhikari P, Zele AJ, Thomas R, Feigl B. Quadrant field pupillometry detects melanopsin dysfunction in glaucoma suspects and early glaucoma. *Sci Rep*. 2016;6:33373.
9. Kankipati L, Girkin CA, Gamlin PD. The post-illumination pupil response is reduced in glaucoma patients. *Invest Ophthalmol Vis Sci*. 2011;52: 2287–2292.
10. Feigl B, Zele AJ. Melanopsin-expressing intrinsically photosensitive retinal ganglion cells in retinal disease. *Optom Vis Sci*. 2014;91:894–903.
11. Maynard ML, Zele AJ, Feigl B. Melanopsin-mediated post-illumination pupil response in early age-related macular degeneration. *Invest Ophthalmol Vis Sci*. 2015;56:6906–6913.
12. Maynard ML, Zele AJ, Kwan AS, Feigl B. Intrinsically photosensitive retinal ganglion cell function, sleep efficiency and depression in advanced age-related macular degeneration. *Invest Ophthalmol Vis Sci*. 2017;58:990–996.
13. Feigl B, Zele AJ, Fader SM, et al. The post-illumination pupil response of melanopsin-expressing intrinsically photosensitive retinal ganglion cells in diabetes. *Acta Ophthalmol*. 2012;90: e230–e234.
14. Park JC, Chen YF, Blair NP, et al. Pupillary responses in non-proliferative diabetic retinopathy. *Sci Rep*. 2017;7:44987.
15. Roecklein K, Wong P, Ernecoff N, et al. The post illumination pupil response is reduced in seasonal affective disorder. *Psychiatry Res*. 2013;210:150–158.
16. Kelbsch C, Maeda F, Lisowska J, et al. Analysis of retinal function using chromatic pupillography in retinitis pigmentosa and the relationship to electrically evoked phosphene thresholds. *Acta Ophthalmol*. 2017;95:e261–e269.
17. Kardon R, Anderson SC, Damarjian TG, Grace EM, Stone E, Kawasaki A. Chromatic pupillometry in patients with retinitis pigmentosa. *Ophthalmology*. 2011;118:376–381.
18. Lisowska J, Lisowski L, Kelbsch C, et al. Development of a chromatic pupillography protocol for the first gene therapy trial in patients with CNGA3-linked achromatopsia. *Invest Ophthalmol Vis Sci*. 2017;58:1274–1282.
19. Kardon RH, Kirkali PA, Thompson HS. Automated pupil perimetry. *Ophthalmology*. 1991;98: 485–496.
20. Schmid R, Lüdtke H, Wilhelm B, Wilhelm H. Pupil campimetry in patients with visual field loss. *Eur J Neurol*. 2005;12:602–608.
21. Skorkovská K, Wilhelm H, Lüdtke H, Wilhelm B. How sensitive is pupil campimetry in hemifield loss? *Graefes Arch Clin Exp Ophthalmol*. 2009; 247:947–953.
22. Naber M, Roelofzen C, Fracasso A, et al. Gaze-contingent flicker pupil perimetry detects scotomas in patients with cerebral visual impairments or glaucoma. *Front Neurol*. 2018;9:558.
23. Chibel R, Sher I, Ben Ner D, et al. Chromatic multifocal pupillometer for objective perimetry and diagnosis of patients with retinitis pigmentosa. *Ophthalmology*. 2016;123:1898–1911.
24. Maddess T, Bedford SM, Goh XL, James AC. Multifocal pupillographic visual field testing in glaucoma. *Clin Exp Ophthalmol*. 2009;37:678–686.
25. Stingl K, Peters T, Strasser T, et al. Pupillographic campimetry: an objective method to measure the visual field. *Biomed Tech (Berl)*. 2018;63:729–734.
26. Skorkovská K, Wilhelm H, Lüdtke H, Wilhelm B, Kurtenbach A. Investigation of summation mechanisms in the pupillomotor system. *Graefes Arch Clin Exp Ophthalmol*. 2014;252:1155–1160.
27. Joyce DS, Feigl B, Zele AJ. Melanopsin-mediated post-illumination pupil response in the peripheral retina. *J Vis*. 2016;16:1–15.
28. Bland J, Altman D. Statistical methods for assessing agreement between two methods of clinical measurement. *Lancet*. 1986;1:307–310.
29. Koch GG. Intraclass correlation coefficient. In: Kotz Is, Johnson NL, eds. *Encyclopedia of Statistical Sciences*. New York: John Wiley & Sons. 1982;213–217.
30. Koo TK, Li MY. A Guideline of selecting and reporting intraclass correlation coefficients for reliability research. *J Chiropr Med*. 2016;15:155–163.
31. Curcio CA, Sloan KR, Kalina RE, Hendrickson AE. Human photoreceptor topography. *J Comp Neurol*. 1990;292:497–523.
32. Legras R, Gaudric A, Woog K. Distribution of cone density, spacing and arrangement in adult healthy retinas with adaptive optics flood illumination. *PLoS One*. 2018;13:e0191141.
33. Barton JJ, Benatar M. *Field of Vision: A Manual and Atlas of Perimetry*. New York: Springer Science & Business Media, 2003.
34. Rosli Y, Bedford SM, James AC, Maddess T. Photopic and scotopic multifocal pupillographic responses in age-related macular degeneration. *Vision Res*. 2012;69:42–48.
35. Davson H. *The Physiology of the Eye*, 3rd ed. New York: Academic Press, 1972.
36. Meins M, Janecke A, Marschke C, et al. Mutations in PDE6A, the Gene Encoding the

α-Subunit of Rod Photoreceptor Cgmp-Specific Phosphodiesterase, are Rare in Autosomal Recessive Retinitis Pigmentosa. In: LaVail MM, Hollyfield JG, Anderson RE, eds. *Degenerative Retinal Diseases*. Boston, MA: Springer, 1997.

37. Haj Yahia S, Hamburg A, Sher I, et al. Effect of stimulus intensity and visual field location on rod- and cone-mediated pupil response to focal light stimuli. *Invest Ophthalmol Vis Sci*. 2018;59: 6027–6035.
38. Kohl S, Marx T, Giddings I, et al. Total colourblindness is caused by mutations in the gene encoding the alpha-subunit of the cone photoreceptor cGMP-gated cation channel. *Nat Genet*. 1998;19:257–259.